Author/s:
Francis, N;Ayodele, BA;O'Brien-Simpson, NM;Birchmeier, W;Pike, RN;Pagel, CN;Mackie, EJ

Title:
Keratinocyte-specific ablation of protease-activated receptor 2 prevents gingival inflammation and bone loss in a mouse model of periodontal disease

Date:
2018-11-01

Citation:
Francis, N., Ayodele, B. A., O'Brien-Simpson, N. M., Birchmeier, W., Pike, R. N., Pagel, C. N. & Mackie, E. J. (2018). Keratinocyte-specific ablation of protease-activated receptor 2 prevents gingival inflammation and bone loss in a mouse model of periodontal disease. Cellular Microbiology, 20 (11), https://doi.org/10.1111/cmi.12891.

Mackie Eleanor Jean (Orcid ID: 0000-0002-8057-5407)

Keratinocyte-specific ablation of protease-activated receptor-2 prevents gingival inflammation and bone loss in a mouse model of periodontal disease

Nidhish Francis[1*], Babatunde A. Ayodele[1], Neil M. O'Brien-Simpson[2], Walter Birchmeier[3], Robert N. Pike[4], Charles, N. Pagel[1#], Eleanor J. Mackie[1#]

[1]Department of Veterinary Biosciences, Melbourne Veterinary School, University of Melbourne, Parkville, Victoria 3010, Australia.

[2]Melbourne Dental School, Bio21 Institute, University of Melbourne, Parkville, Victoria 3010, Australia

[3]Max-Delbrück-Center for Molecular Medicine, 13125 Berlin, Germany

[4]La Trobe Institute for Molecular Science, La Trobe University, Bundoora, Victoria 3086, Australia

[*] Current address: School of Animal and Veterinary Sciences, Charles Sturt University, Wagga Wagga, NSW 2650, Australia

[#] The last two authors made equal contributions to the manuscript

Corresponding author:

Prof. E.J. Mackie

Department of Veterinary Biosciences, Melbourne Veterinary School, Faculty of Veterinary and Agricultural Sciences, University of Melbourne, Parkville, Victoria 3010, Australia

Tel: +61 3 8344 7360

This is the author manuscript accepted for publication and has undergone full peer review but has not been through the copyediting, typesetting, pagination and proofreading process, which may lead to differences between this version and the Version of Record. Please cite this article as doi: 10.1111/cmi.12891

Email: ejmackie@unimelb.edu.au

ABSTRACT

Chronic periodontitis is characterised by gingival inflammation and alveolar bone loss. A major aetiological agent is *Porphyromonas gingivalis*, which secretes proteases that activate protease-activated receptor-2 (PAR_2). PAR_2 expressed on oral keratinocytes is activated by proteases released by *P. gingivalis*, inducing secretion of interleukin-6 (IL-6), and global knockout of PAR_2 prevents bone loss and inflammation in a periodontal disease model in mice. To test the hypothesis that PAR_2 expressed on gingival keratinocytes is required for periodontal disease pathology, keratinocyte-specific PAR_2-null mice were generated using K14-Cre targeted deletion of the PAR_2 gene (*F2rl1*). These mice were subjected to a model of periodontitis involving placement of a ligature around a tooth, combined with *P. gingivalis* infection ('Lig+Inf'). The intervention caused a significant 44% decrease in alveolar bone volume (assessed by micro-computed tomography) in wildtype (*K14-Cre:F2rl1*$^{wt/wt}$), but not littermate keratinocyte-specific PAR_2-null (*K14-Cre:F2rl1*$^{fl/fl}$) mice. Keratinocyte-specific ablation of PAR_2 prevented the significant Lig+Inf-induced increase (2.8-fold) in the number of osteoclasts in alveolar bone and the significant up-regulation (2.4-4-fold) of the inflammatory markers IL-6, IL-1β, interferon-γ, myeloperoxidase and CD11b in gingival tissue. These data suggest that PAR_2 expressed on oral epithelial cells is a critical regulator

of periodontitis-induced bone loss and will help in designing novel therapies with which to treat the disease.

INTRODUCTION

The pathophysiology of chronic periodontitis involves establishment of a chronic inflammatory state in the gingiva, which leads to resorption of alveolar bone and ultimately tooth loss. The process is initiated by infection with bacteria including *Porphyromonas gingivalis*, which relies on production of a group of cysteine proteases known as the gingipains for its pathogenicity (Bostanci & Belibasakis, 2012). Both the arginine-specific gingipain B (RgpB) and the lysine-specific gingipain (Kgp) activate the G-protein-coupled receptor, protease-activated receptor-2 (PAR_2; (Lourbakos *et al.*, 1998, Liu *et al.*, 2017). This receptor is expressed by many cells present in the normal periodontal tissues, including oral epithelial cells, gingival fibroblasts, osteoblasts and osteoclast precursors, as well as the neutrophils, macrophages, mast cells and lymphocytes that are present once inflammation is established (Lourbakos *et al.*, 1998, Lourbakos *et al.*, 2001, Abraham *et al.*, 2000, Bar-Shavit *et al.*, 2002, Belibasakis *et al.*, 2010, D'Andrea *et al.*, 2000, Smith *et al.*, 2004).

Agonists of PAR_2 can induce periodontal disease in rats when applied topically, and PAR_2 is required for normal bone loss in a model of periodontal disease induced by *P. gingivalis*, as demonstrated in mice in which the PAR_2 gene was deleted globally

(Holzhausen *et al.*, 2006, Holzhausen *et al.*, 2005, Wong *et al.*, 2010). While these studies highlighted the importance of PAR_2 as a mediator of periodontal disease, they could not identify the critical PAR_2-expressing cells, since PAR_2 was absent from all cells in these mice. In global PAR_2-null mice subjected to *P. gingivalis*-induced periodontal disease, T lymphocyte responses to the pathogen were defective, suggesting that these cells may require PAR_2 for their contributions to the condition (Wong *et al.*, 2010). We have recently generated a mouse line in which PAR_2 was selectively ablated from T lymphocytes under the control of the *Lck* promoter (Francis *et al.*, 2017). In these mice, T lymphocyte development was perturbed, suggesting that the aberrant T lymphocyte responses in global PAR_2-null mice may result from the abnormal phenotype of these cells, rather than a requirement for PAR_2 on mature T cells.

We have previously demonstrated that activation of PAR_2 on oral epithelial cells by RgpB stimulates secretion of the pro-inflammatory cytokine interleukin-6 (IL-6; (Lourbakos *et al.*, 2001). This observation led to the hypothesis that PAR_2 on oral epithelial cells plays a critical role in the initiation of periodontal disease, since these are the first cells that come in contact with periodontal pathogens including *P. gingivalis* as they invade the gingiva. Based on this hypothesis, we have developed a model describing the role of PAR_2 in the pathophysiology of periodontal disease. According to our model, IL-6, and possibly other factors released from oral epithelial cells in response to PAR_2 activation, causes infiltration of the gingiva by inflammatory cells (neutrophils, macrophages, lymphocytes and mast cells). These cells also express PAR_2 and secrete cytokines and/or PAR_2–activating proteases, thus amplifying the inflammation. Consequently, the presence of cytokines (including IL-1, IL- 6,

IL-17 and receptor activator of NF-κB ligand; RANKL) that stimulate differentiation and activity of the bone-resorbing osteoclasts ultimately leads to loss of alveolar bone (Kayal, 2013, Wong *et al.*, 2010).

In order to test our hypothesis, we have generated a mouse line in which PAR_2 is deleted from keratinocytes (including oral epithelial cells). Here we present the results of our studies investigating the responses of these mice to a model of periodontal disease.

RESULTS

Characterisation of keratinocyte-specific PAR_2-null mice

Quantitative PCR analysis of exon 2 of *F2rl1* in genomic DNA isolated from keratinocytes from the skin of newborn mice demonstrated that the abundance of the coding sequences of this gene in the keratinocytes of keratinocyte-specific PAR_2-null (*K14-Cre:F2rl1*$^{fl/fl}$) mice was 94% lower than in those of their littermate wildtype (*K14-Cre:F2rl1*$^{wt/wt}$) controls (Fig. 1A). Expression of *F2rl1* transcripts was also significantly lower (95%) in keratinocytes from *K14-Cre:F2rl1*$^{fl/fl}$ mice as compared with those from *K14-Cre:F2rl1*$^{wt/wt}$ mice (Fig. 1A).

Intracellular calcium mobilisation assays demonstrated that while treatment of keratinocytes from *K14-Cre:F2rl1*$^{fl/fl}$ mice with the positive control, ATP, resulted in a normal response, these cells showed no response to either of the PAR_2-activating peptides (2-furoyl-LIGRLO-NH_2 and SLIGRL-NH_2), at concentrations that yielded responses in *K14-Cre:F2rl1*$^{wt/wt}$ mice (Fig. 1B). Dermal fibroblasts from *K14-Cre:F2rl1*$^{fl/fl}$ mice were, however, able to respond normally to the PAR_2-activating peptides (Fig. 1B).

Combined ligature and infection model of periodontal disease in global PAR_2-null and control strains of mice

Initial experiments were undertaken to confirm that the periodontal disease model combining application of a ligature to the second maxillary molar tooth with oral infection by *P. gingivalis* (the 'Lig+Inf' model) was appropriate for use in *K14-Cre:F2rl1*$^{fl/fl}$ mice. Global PAR_2-null (*F2rl1*$^{-/-}$), non-Cre PAR_2 'floxed' (*F2rl1*$^{fl/fl}$) and wildtype (*F2rl1*$^{wt/wt}$) mice were subjected to either Lig+Inf or sham treatment. Lig+Inf mice of all genotypes showed evidence of establishment of *P. gingivalis* infection, as demonstrated by both isolation of the bacteria from oral mucosa (detected by qPCR) and the presence of anti-*P. gingivalis* IgG in serum at the end of the experiment (Fig. 2A).

The alveolar BV/TV, as assessed by microCT, was significantly reduced by Lig+Inf in both the *F2rl1*$^{wt/wt}$ and *F2rl1*$^{fl/fl}$ genotypes, whereas no significant change was observed in *F2rl1*$^{-/-}$, mice (Fig. 2B). In agreement with this observation, osteoclast numbers in alveolar bone were increased by Lig+Inf in both the *F2rl1*$^{wt/wt}$ and *F2rl1*$^{fl/fl}$ genotypes, whereas no significant change was observed in *F2rl1*$^{-/-}$, mice (Fig. 2C). The number of mast cells in the periodontal soft tissues was also significantly elevated in response to Lig+Inf in *F2rl1*$^{wt/wt}$ and *F2rl1*$^{fl/fl}$ mice, but not in *F2rl1*$^{-/-}$ mice (Fig. 2D). In comparisons between mice of different genotypes in the Lig+Inf treatment group, the values for BV/TV were significantly higher in *F2rl1*$^{-/-}$ mice than in both the *F2rl1*$^{wt/wt}$ and *F2rl1*$^{fl/fl}$ genotypes, and mast cell numbers were significantly lower in *F2rl1*$^{-/-}$ than in *F2rl1*$^{wt/wt}$ mice.

Expression of a number of inflammation-associated genes was analysed by qPCR in periodontal soft tissues collected at the end of the experiment. Expression of genes encoding

IL-1β (*Il1b)*, IL-6 *(Il6)*, interferon-γ (*Ifng*), myeloperoxidase (*Mpo*), inducible nitric oxide synthase (*Nos2*) and CD11b (*Cd11b*) was upregulated by Lig+Inf treatment in mice of the two PAR_2-expressing genotypes (*F2rl1*$^{wt/wt}$ and *F2rl1*$^{fl/fl}$), but not in *F2rl1*$^{-/-}$ mice (Fig. 3). Expression of the gene encoding transforming growth factor-β1 was up-regulated in all three genotypes, and expression of those encoding macrophage inflammatory protein-2 (*Cxcl2*) and tumour necrosis factor-α was not affected in any genotype (data not shown). In comparisons between mice of different genotypes in the Lig+Inf treatment group, the values for all of these genes were significantly lower in *F2rl1*$^{-/-}$ mice than in both the *F2rl1*$^{wt/wt}$ and *F2rl1*$^{fl/fl}$ genotypes, with the exception of that of *Cd11b*, which was lower in *F2rl1*$^{-/-}$ than in *F2rl1*$^{fl/fl}$ mice.

Use of keratinocyte-specific PAR_2-null mice in the periodontal disease model

When *K14-Cre:F2rl1*$^{wt/wt}$ and *K14-Cre:F2rl1*$^{fl/fl}$ mice were subjected to the periodontal disease model, the Lig+Inf groups for both genotypes showed evidence of infection with *P. gingivalis*, through detection of both bacteria and antibodies to them (Fig. 4A).

Alveolar bone loss was induced by Lig+Inf in *K14-Cre:F2rl1*$^{wt/wt}$, but not *K14-Cre:F2rl1*$^{fl/fl}$ mice, as demonstrated by microCT assessment of BV/TV (Fig. 4B). The number of osteoclasts in alveolar bone was elevated in response to Lig+Inf in *K14-Cre:F2rl1*$^{wt/wt}$, but not *K14-Cre:F2rl1*$^{fl/fl}$, mice. An increase in the number of mast cells in the periodontal soft tissues in response to Lig+Inf was, however, observed in both *K14-Cre:F2rl1*$^{wt/wt}$ and *K14-Cre:F2rl1*$^{fl/fl}$ mice (Fig. 4D). While serum IL-6 was elevated by Lig+Inf in *K14-Cre:F2rl1*$^{wt/wt}$ mice, no increase was observed in *K14-Cre:F2rl1*$^{fl/fl}$ mice (Fig.

4E). In comparisons between mice of different genotypes in the Lig+Inf treatment group, the values for BV/TV were significantly higher in *K14-Cre:F2rl1*$^{fl/fl}$ than in *K14-Cre:F2rl1*$^{wt/wt}$ mice, and serum IL-6 levels were significantly lower in *K14-Cre:F2rl1*$^{fl/fl}$ than in *K14-Cre:F2rl1*$^{wt/wt}$ mice.

As observed for *F2rl1*$^{wt/wt}$ and *F2rl1*$^{fl/fl}$ mice, six inflammation-associated genes were upregulated in the gingiva of *K14-Cre:F2rl1*$^{wt/wt}$ mice (Fig. 5). In contrast to the results obtained for *F2rl1*$^{-/-}$ mice, however, in *K14-Cre:F2rl1*$^{fl/fl}$ mice, abrogation of up-regulation in response to Lig+Inf was only observed for five of the six inflammation-associated genes (Fig. 5). The gene encoding iNOS was significantly up-regulated by Lig+Inf in *K14-Cre:F2rl1*$^{fl/fl}$ mice. In comparisons between mice of different genotypes in the Lig+Inf treatment group, the values for all of these genes were significantly lower in *K14-Cre:F2rl1*$^{fl/fl}$ than in *K14-Cre:F2rl1*$^{wt/wt}$ mice, with the exception of that of *Nos2*, for which there was no significant difference between genotypes.

DISCUSSION

We have generated keratinocyte-specific PAR_2-null mice in order to identify the role of PAR_2 expressed by oral epithelial cells in periodontal disease. Our characterisation of the mice demonstrated that functional ablation of PAR_2 was achieved specifically in keratinocytes, confirming that it was appropriate to use these mice to investigate our hypothesis.

In our previous study of periodontal disease in global PAR_2-null mice, a model of periodontal disease dependent solely on oral infection with *P. gingivalis* was used, which

requires 8 weeks from the time of initial infection until the mice are killed (Wong *et al.*, 2010). In the current study, we chose to accelerate the pathology by combining the use of a ligature applied to the second maxillary molar teeth with oral *P. gingivalis* infection, allowing us to shorten the experimental period to 4 weeks, as described by (Lin *et al.*, 2014). Initial experiments involved confirmation that this model was appropriate for the study of cell-type specific PAR_2-null mice. This was achieved through the demonstration both that the alveolar bone loss and periodontal inflammation associated with periodontal disease were abrogated by global PAR_2 knockout (i.e. in *F2rl1*$^{-/-}$ mice), and that they occurred normally in the PAR_2 floxed (*F2rl1*$^{fl/fl}$) mice that we were planning to use to generate cell type-specific PAR_2-null mouse lines.

The phenotype of *K14-Cre:F2rl1*$^{fl/fl}$ mice subjected to the periodontal disease model mimicked that of *F2rl1*$^{-/-}$ mice in most of the assays undertaken. Importantly, the destructive bone loss, which eventually leads to tooth loss in human periodontal disease patients, was prevented by ablation of PAR_2 expression in keratinocytes. Thus, it appears that activation of PAR_2 on oral epithelial cells, most likely by gingipains released by *P. gingivalis*, is sufficient to initiate an inflammatory cascade ultimately leading to stimulation of osteoclast differentiation and activity. Evidence of induction of gingival inflammation by Lig+Inf in all the mouse strains with normal PAR_2 expression (*F2rl1*$^{wt/wt}$, *F2rl1*$^{fl/fl}$ and *K14-Cre:F2rl1*$^{wt/wt}$) was demonstrated by upregulation of the inflammatory cytokine genes *Il1b*, *Il6* and *Ifng*, as well as *Mpo*, which is primarily expressed by neutrophils, and *Nos2* and *Cd11b*, both of which are expressed by a variety of leukocytes, including neutrophils, macrophages, lymphocytes and mast cells, all of which are cells known to contribute to the pathology of

periodontal disease (Malcolm *et al.*, 2016, Kayal, 2013). Moreover, periodontal mast cell numbers were increased by Lig+Inf in all these mouse strains. In contrast, none of these parameters was increased by Lig+Inf in *F2rl1*$^{-/-}$ mice and none except *Nos2* expression and mast cell numbers was increased in *K14-Cre:F2rl1*$^{fl/fl}$ mice.

Thus, it appears that while deletion of PAR_2 on keratinocytes is sufficient to prevent most aspects of the inflammation observed in periodontal disease, it has no impact on gingival mast cell infiltration or *Nos2* expression, indicating that these two parameters require PAR_2 expression by another cell type. We previously described the lack of mast cell infiltration into the periodontal tissues of *F2rl1*$^{-/-}$ mice infected orally with *P. gingivalis*, and on the basis of the observations proposed that PAR_2 expressed by mast cells is required for their infiltration (Wong *et al.*, 2010). Thus, the PAR_2–expressing cells that allow for mast cell infiltration in keratinocyte-specific, but not global PAR_2-null, mice may be the mast cells (or their precursors) themselves. However, it is also worth considering the identity of the protease(s) available for activation of PAR_2 in the gingiva of keratinocyte-specific PAR_2-null mice. We previously proposed that following initiation of the inflammatory response by gingipains activating PAR_2 on gingival epithelial cells, the response is amplified by PAR_2-activating proteases secreted by the invading inflammatory cells, which in turn activate PAR_2 on the inflammatory cells in an autocrine and/or paracrine manner (Wong *et al.*, 2010). Such proteases include granzyme A (from lymphocytes), neutrophil elastase and mast cell tryptase (Adams *et al.*, 2011, Ramachandran *et al.*, 2011). However, in the absence of the normal inflammatory response in *K14-Cre:F2rl1*$^{fl/fl}$ mice, these sources of host proteases are most likely not available prior to mast cell infiltration. The *P. gingivalis*-derived gingipains are

present (at the gingival surface, at least), and it is likely that their activation of PAR_2 on another normal gingival cell population such as fibroblasts leads to release of a chemoattractant for mast cells. For example, hepatocyte growth factor (HGF), secretion of which by gingival fibroblasts is stimulated in a PAR_2–dependent manner by gingipains, stimulates migration of mouse bone marrow-derived mast cells *in vitro* (Uehara *et al.*, 2005, Fehlner-Gardiner *et al.*, 1999); this may be the mechanism by which mast cells are attracted to the gingiva of mice lacking PAR_2 in their oral epithelium.

Activation of PAR_2 on mast cells leads to the release of inflammatory mediators, and we have proposed that this effect may contribute to periodontal disease pathology (Wong *et al.*, 2010, Alshurafa *et al.*, 2004, Carvalho *et al.*, 2010, Moormann *et al.*, 2006). More recently, a study in mast cell-deficient mice demonstrated that these cells are required for *P. gingivalis*-induced alveolar bone loss (Malcolm *et al.*, 2016). The results of the current study indicate, however, that the presence of PAR_2-expressing mast cells is not sufficient to cause alveolar bone loss in the absence of other important contributors to periodontal inflammation. It seems likely that what is missing in keratinocyte-specific PAR_2-null mice exposed to Lig+Inf treatment is other inflammatory cells, which when available may act as mediators of mast cell-induced bone loss.

Up-regulation of *Nos2/NOS2* in periodontal tissues in association with periodontal disease has been described in both animal models and human patients (Lohinai *et al.*, 1998, Lappin *et al.*, 2000). As noted above, *Nos2* is expressed by a variety of leukocytes. Due to the small amount of available material from each mouse, it was not possible in the current study to undertake immunohistochemical analysis of all of these cell types, but the fact that

neither *Mpo* nor *Cd11b* was upregulated by Lig+Inf in *K14-Cre:F2rl1*$^{fl/fl}$ mice suggests that there was minimal infiltration of the periodontal tissues by inflammatory cells other than mast cells in these mice. It appears likely, therefore, that mast cells were responsible for the *Nos2* expression. Inhibition of inducible nitric oxide synthase in a rat model of periodontal disease led to a decrease in alveolar bone loss (Herrera *et al.*, 2011). However, in the current study, despite up-regulation of *Nos2* in the gingiva of *K14-Cre:F2rl1*$^{fl/fl}$ mice, there was no concomitant stimulation of alveolar bone loss, suggesting that *Nos2* expression is not sufficient to initiate alveolar bone loss in the absence of factors that are dependent on PAR_2 expressed on keratinocytes. Inducible nitric oxide synthase is required for IL-1-induced osteoclastic bone resorption, but nitric oxide does not induce osteoclast differentiation in the absence of IL-1 (van't Hof *et al.*, 2000); since *Il1b* was up-regulated by Lig+Inf in the gingiva of *K14-Cre:F2rl1*$^{wt/wt}$ but not *K14-Cre:F2rl1*$^{fl/fl}$ mice, it is not surprising that *Nos2* expression alone was insufficient to induce alveolar bone loss.

We have previously demonstrated that gingipains stimulate secretion of IL-6 by oral keratinocytes *in vitro* (Lourbakos *et al.*, 2001), and according to our hypothesis, this IL-6 (and perhaps other inflammatory mediators) plays a critical role in attracting inflammatory cells to the site of *P. gingivalis* infection. Oral keratinocytes are probably not the only cells responsible for the IL-6 detected in the serum of Lig+Inf mice four weeks after initiation of periodontal disease; other cells present in inflamed periodontal tissues that are known to express IL-6 include neutrophils, lymphocytes and macrophages (Lundqvist *et al.*, 1994, Grenier & Grignon, 2006, Shpacovitch *et al.*, 2004). It is likely that in mice with normal PAR_2 expression, a combination of these cell types contributes to the elevated IL-6 detected

in serum. Circulating IL-6 levels in patients with periodontitis are higher than in healthy controls and decrease with treatments that lead to clinical improvement, and it has been suggested that this IL-6 may contribute to the association between periodontitis and other chronic conditions including cardiovascular disease and diabetes (D'Aiuto *et al.*, 2004, Loos *et al.*, 2000). Intriguingly, although the systemic and local chemokine/cytokine responses and bone loss were abrogated in Lig+Inf *K14-Cre:F2rl1*$^{fl/fl}$ mice in comparison to the Lig+Inf controls (*K14-Cre:F2rl1*$^{wt/wt}$ mice), the levels of *P. gingivalis* infection in the gingiva were equivalent. This suggests that a typical periodontal plaque biofilm has been established in all Lig+Inf animals. Thus, it appears that a key interaction is the activation of PAR_2 on gingival keratinocytes by the gingipains released by *P. gingivalis* in the dental plaque biofilm. We could therefore speculate that bacterial burden alone is not enough to trigger disease pathology, however we cannot rule out the possibility that keratinocyte-specific PAR_2 signalling in response to *P. gingivalis* proteases influences other components of the biofilm. Our observation that inactivation of PAR_2 on keratinocytes alone can prevent this systemic manifestation of periodontal disease provides hope that targeted therapies can be developed that not only prevent bone (and therefore tooth) loss, but also the associated systemic conditions.

It may seem contradictory that *Ifng* up-regulation in gingival tissue is dependent on the presence of PAR_2 on keratinocytes, since we previously demonstrated that PAR_2-activating proteases including RgpB do not stimulate secretion of interferon-γ in cultured oral keratinocytes (Lourbakos *et al.*, 2001). However, the gingival tissue used for quantitation of gene expression in the current study comprised connective tissue and any inflammatory

infiltrate in addition to the epithelial component. Inflammatory cells, the presence of which is dependent on keratinocyte PAR_2, are the most likely source of the up-regulated *Ifng*.

Gingipains are not the only enzymes from *P. gingivalis* required for its ability to induce alveolar bone loss. Peptidylarginine deiminase (PAD) is also required, as demonstrated by a study involving infection of mice with PAD-deficient *P. gingivalis* (Gully *et al.*, 2014). This enzyme catalyses the citrullination of peptides, however serum from mice infected with control (PAD-expressing) *P. gingivalis* did not contain elevated levels of serum anti-citrullinated protein antibodies, thus the mechanism of induction of alveolar bone loss by *P. gingivalis* PAD is unclear. It is likely that both of these groups of *P. gingivalis* enzymes act in the same pathway, i.e. one downstream from the other, since inactivation of each one individually (deletion of PAD from *P. gingivalis* and deletion of PAR_2 from the host) is able to prevent bone loss.

The results presented here provide evidence supporting our hypothesis that PAR_2 on oral epithelial cells plays a critical role in the initiation of periodontal disease, and allow us to refine our model of the role of PAR_2 in the pathophysiology of periodontal disease (Fig. 6). According to the model, *P. gingivalis* proteases activate PAR_2 on gingival keratinocytes, resulting in secretion of IL-6 and possibly other inflammatory mediators, which in turn either directly or indirectly recruit inflammatory cells to the gingiva; these cells most likely include neutrophils, macrophages and lymphocytes, but not mast cells, which are able to accumulate in the absence of keratinocyte PAR_2. The keratinocyte PAR_2-dependent inflammatory cells secrete cytokines including IL-1β, IFN-γ and more IL-6. Moreover, T lymphocytes in inflamed periodontal tissues are known to secrete the osteoclastogenic factors IL-17 and

RANKL (Kayal, 2013). These factors would collectively amplify the inflammatory response and stimulate osteoclast differentiation and bone resorption. While mast cell infiltration is not dependent on gingival keratinocyte PAR_2 expression, it is dependent on global PAR_2 expression, indicating the existence of a second PAR_2-dependent pathway that contributes to gingival inflammation but is not sufficient to induce alveolar bone loss. In conclusion, as well as identifying a critical role for keratinocyte-specific PAR_2 expression in bone loss in the context of periodontal disease, the results presented here demonstrate that although mast cells are necessary (Malcolm *et al.*, 2016), they are not sufficient for bone loss in periodontal disease.

EXPERIMENTAL PROCEDURES

Materials

Reagents for cell culture were from GIBCO-ThermoFisher Scientific (Waltham, MA, USA) unless otherwise stated. Hyclone™ foetal bovine serum (FBS) was from ThermoFisher Scientific. Chemicals were from Sigma-Aldrich (St Louis, MO, USA) unless otherwise stated. Reagents for RNA extraction, reverse transcription and polymerase chain reaction (PCR) were from Promega (Madison, WI, USA). Oligonucleotide primers were custom synthesised by Geneworks (Thebarton, SA, Australia). Peptide agonists of PAR_2 were custom synthesised by Sigma-Aldrich. The *P. gingivalis* strain W50 (American Type Culture Collection, Manassas, VA, USA) was grown and prepared for mouse infection studies as described (O'Brien-Simpson *et al.*, 2000b, O'Brien-Simpson *et al.*, 2001). Heat-killed *P. gingivalis* strain W50 (HKW50) was prepared as described (Palm *et al.*, 2013).

Animals

Mice with global deletion of the gene encoding PAR_2 (*F2rl1*$^{-/-}$ mice; (Lindner *et al.*, 2000) were obtained from Dr S. R. Coughlin (University of California, San Francisco). The generation of mice with LoxP sites flanking exon 2 of the gene encoding PAR_2 (*F2rl1*$^{fl/fl}$ mice) has been described (Francis *et al.*, 2017). These mice were crossed with mice expressing Cre-recombinase under the control of the keratin 14 (*K14*) promoter (*K14-Cre:F2rl1*$^{wt/wt}$ mice; (Huelsken *et al.*, 2001) to generate keratinocyte-specific PAR_2–null (*K14-Cre:F2rl1*$^{fl/fl}$) mice. Mouse colonies were maintained as heterozygous breeding stock, thus all experimental mice were littermates or the offspring of littermates.

The use of animals in this study was approved by the Gene Technology and Biosafety Committee of the University of Melbourne and the Animal Ethics Committee of the Faculty of Veterinary and Agricultural Sciences (AEC 1212655 and 1312922). Mice were housed in a controlled environment with free access to food and water, and all work was conducted in compliance with the Australian Code for the Care and Use of Animals for Scientific Purposes (2013) and the National Health and Medical Research Council's Guidelines for the Generation, Breeding, Care and Use of Genetically Modified and Cloned Animals for Scientific Purposes (2007).

Cell culture

Keratinocytes and dermal fibroblasts were isolated from the skin of newborn mice as described (Lichti *et al.*, 2008). This method involved separation of the two cell types following floating of the skin overnight on trypsin (0.25% [w/v]; 4°C). Isolated

keratinocytes were cultured in low calcium (0.12 mM) Clonetics™ keratinocyte growth medium (KGM-2; Lonza, Basel, Switzerland) and dermal fibroblasts were cultured in Dulbecco's modified Eagle's medium containing FBS (10% [v/v]), L-glutamine (300 μg/mL), gentamicin (50 μg/mL) and amphotericin B (2.5 μg/mL); cells were cultured in 96-well plates ($3x10^4$ cells/well) for calcium mobilisation assays or in 35 mm dishes for extraction of RNA or genomic DNA.

Polymerase chain reaction

RNA was extracted from cultured cells and mouse tissues using Wizard SV RNA extraction columns (Promega, Madison, WI, USA). Genomic DNA was extracted from mouse ear clips (for genotyping of pups at weaning) using the HotSHOT genomic DNA extraction method (Truett *et al.*, 2000) and from cultured cells using Wizard SV DNA purification columns (Promega) according to the manufacturer's instructions. First-strand cDNA was synthesised from purified RNA using the GoScript reverse transcription system (Promega).

Polymerase chain reaction was performed on template DNA in 20 μl total reaction volume containing forward and reverse oligonucleotide primers (1 μM each; Geneworks, Hindmarsh, SA, Australia; (Pagel *et al.*, 2003). Primers for genotyping and quantitation of PAR_2 exon 2 and GAPDH in genomic DNA (Francis *et al.*, 2017), and PAR_2 and cyclophilin A in RNA (Georgy *et al.*, 2010) were as described; the other primers used were designed using Primer3 software (http://bioinfo.ut.ee/primer3/; Table 1), and their specificity confirmed by sequencing of transcripts. Thermal cycling was conducted over 35 cycles

(95°C for 30 s, 56°C for 30 s and 72°C for 30 s), prior to resolution of amplified products on agarose gels in the presence of SYBR Safe (Life Technologies, Grand Island, NY USA).

Quantitative PCR (qPCR) was performed on an MX3000p Real Time PCR Machine. PCR reactions containing 10 µl ABI SYBR Green Supermix, 250 nM each forward and reverse primer and 1 µl cDNA or genomic DNA template, were incubated using the following cycle profile: 95°C for 10 min, followed by 40 cycles consisting of 95°C for 30 s, 60°C for 30 s and 72°C for 30 s. Fluorescence readings were acquired at the end of each extension step in the FAM/SYBR channel of the machine. Following amplification, values for the cycle threshold (Ct) for each primer pair and sample were exported to Microsoft Excel and analyzed using the Q-Gene tool (Simon, 2003). The Q-gene tool gives results as mean normalised expression (MNE; mean abundance normalised to a housekeeping gene), thus data for mRNA expression are presented as MNE (normalised to cyclophilin A) and data for PAR_2 coding sequences in mouse cell genomic DNA are presented as mean abundance (normalised to GAPDH coding sequences).

Calcium mobilisation

Twenty-four hours after plating, cells were washed in assay buffer (Hanks' balanced salt solution containing 0.1% [w/v] bovine serum albumin) then incubated in assay buffer containing probenecid (2.5 mM), Fura-2 AM (1 µM; Molecular Probes, Life Technologies) and pluronic acid (0.01 % [v/v]) for 1 h at 37°C. Following incubation, cells were washed twice with the assay buffer and incubated in assay buffer. The fluorescent emission at 510 nm after excitation at 340 and 380 nm was measured using a Flexstation 3 Multi-Mode microplate reader (Molecular Devices, Sunnyvale CA). Sixty seconds after commencement

of the reading, PAR_2 agonist (2-furoyl-LIGRLO-NH_2 [10 μM] or SLIGRL-NH_2 [100 μM]), the positive control (ATP [10 μM]) or the negative control (assay buffer) was injected into each well. The intracellular calcium concentration was expressed as the ratio of the emission at 510 nm following excitation at 340 and 380 nm, respectively.

Periodontal disease model

A periodontal disease model involving a combination of application of a ligature to a tooth and infection with *P. gingivalis* was used. The experimental regimen was similar to that described by (Lin *et al.*, 2014), with the exception that we administered more doses of *P. gingivalis*. Female mice (8-10 weeks old) of all genotypes were randomly assigned to either ligature and infection ('Lig+Inf') or sham groups. Mice were anaesthetized by intraperitoneal injection of ketamine (100 mg/kg body weight; Troy Laboratories, Glendenning, NSW, Australia) and xylazine (10 mg/kg body weight; Troy Laboratories), then a ligature was tied around left and right second maxillary molar teeth as described (Abe & Hajishengallis, 2013). Commencing the next day, *P. gingivalis* strain W50 (1×10^{10} bacterial cells in 2% [w/v] carboxymethyl cellulose [CMC]/dose) was administered topically to the gingiva every two days four times, followed by a 10-day break, then another four times two days apart. Mice assigned to the sham group received no ligature; they received 2% CMC without bacteria when the mice assigned to the Lig+Inf group received bacteria. Mice were killed 4 weeks after the placement of ligatures, then blood was collected by cardiac puncture for serum preparation, a sterile paper point was placed against the gingival margin of each maxilla for bacterial culture, and maxillae were excised and divided into halves. The gingiva surrounding the right half maxilla was removed and snap frozen in liquid nitrogen;

the remaining bone was defleshed as described (Pathirana *et al.*, 2007). The left half maxilla (with intact gingival tissue) was placed in 4% (w/v) paraformaldehyde in phosphate-buffered saline (PBS) for preparation of cryosections. Submandibular lymph nodes were harvested for isolation of T cells.

Paper points were used for culture of recovered *P. gingivalis* for two days, as described (Baker *et al.*, 2000). DNA was extracted from the bacterial samples for quantitation of bacteria using quantitative PCR as described (Pathirana *et al.*, 2007). Standard curves using DNA isolated from pure cultures of *P. gingivalis* were generated for *P. gingivalis* 16S rDNA and for a universally conserved region of 16S rDNA. Results are presented as *P. gingivalis* 16S rDNA as a percentage of total bacterial 16S rDNA in the same sample.

Serum was used to detect anti-*P. gingivalis* IgG by ELISA as described (O'Brien-Simpson *et al.*, 2000a) as well as IL-6 using an ELISA kit according to the manufacturer's instructions (R&D Systems, Minneapolis, MN, USA).

Micro-computed tomography

To assess alveolar bone loss, the bone volume fraction (bone volume/tissue volume; BV/TV) of the alveolar bone on the buccal aspect of the three right maxillary molar teeth was measured from micro-computed tomography (microCT) images. Images of de-fleshed half maxillae were obtained using a Scanco microCT 50 at 70 kV, 85 µA, 18 μm^3 voxel and 0.5 mm aluminium filter (Scanco Medical, Brüttisellen, Switzerland). The 2D image sets were realigned such that the cemento-enamel junction (CEJ), the roof of furcation and the root apex of all molars are visible on the same sagittal image (using ImageJ version 1.5;

https://imagej.nih.gov). The images were then reoriented in the dorsal plane, along the line connecting the CEJ of the first and third molar teeth, to draw a region of interest. Measurements were undertaken by an operator blinded to the treatment groups (sham or Lig+Inf). For each maxilla, the distance from the CEJ to the alveolar bone crest (ABC) at the distal border of the second molar was estimated, and for each genotype the minimum and maximum CEJ-ABC distances were determined, representing no bone loss and maximum bone loss, respectively. The BV/TV of each sample was measured using all dorsal slices falling between the minimum and maximum CEJ-ABC distances. The mesial border of the region of interest was defined as a line drawn in each slice perpendicular to the mesial surface of the first molar, and the distal border was defined as a line adjacent to the distal surface of the third molar roots (see Supplementary Figure 1). Voxels attributable to bone within this region of interest in all slices were used to calculate BV/TV.

Histology

Following overnight incubation in fixative, left half maxillae were demineralised and processed for preparation of cryosections as described (Campbell *et al.*, 2003). Sagittal sections (8-10 μm) were cut using a cryostat (Leica CM 1900, Wetzlar, Germany). Sections were post-fixed in 4% (w/v) paraformaldehyde in PBS for 5 minutes at room temperature prior to staining. Some sections were stained for the presence of the osteoclast-specific enzyme tartrate-resistant acid phosphatase (TRAP) by incubating with freshly prepared TRAP stain consisting of sodium tartrate (30 mM), naphthol AS-MX phosphate (0.1 mg/ml), triton X-100 (0.1% v/v) and fast red violet LB (0.3 mg/ml) in acetate buffer (0.05 M) at room temperature for 10 minutes. After colour development, sections were rinsed with water,

counterstained with Carazzi's haematoxylin and mounted in gelvatol. Some sections were stained with toluidine blue (1% in 70% ethanol; 15 seconds), dehydrated and mounted in DPX. Sections were examined by brightfield microscopy (BX60; Olympus, Tokyo, Japan) and images were collected using a digital camera (Retiga 6000; QImaging, Surrey, BC, Canada). The area of alveolar bone extending from a vertical line touching the mesial surface of the first molar to a vertical line touching the distal surface of the third molar was measured using ImageJ. Osteoclasts were counted as TRAP-positive cells adherent to bone surfaces and containing more than two nuclei; results are presented as osteoclasts/mm^2 of bone. Mast cells, identified by their metachromatic granules in toluidine blue-stained sections, were counted in the gingival and periodontal connective tissue; results are presented as mast cells/mm^2 of soft tissue (measured using Image J).

Statistical analysis

Data were analysed using GraphPad Prism software (version 5.01; La Jolla, CA, USA). Mean and standard error of the mean (SEM) are presented (as well as individual data points) in all graphs. Quantitative PCR data (where expressed as MNE) were analysed for significant differences by a pairwise fixed reallocation randomisation test, using REST-384 software (Pfaffl *et al.*, 2002). Other data were analysed by unpaired Student's t-test for comparisons between two groups or ANOVA for multiple comparisons; Mann Whitney test or Kruskal-Wallis test with Dunn's multiple comparison test were used for data that were not normally distributed. P values < 0.05 were considered significant.

ACKNOWLEDGMENTS

This work was supported by the National Health and Medical Research Council of Australia (project grant number 1044103). Nidhish Francis was supported by a Victoria India Doctoral Scholarship. The authors wish to thank Prof. Jan Potempa and Dr Malgorzata Benedyk (Jagiellonian University, Krakow, Poland) for training in application of ligatures to mouse molar teeth, and Prof. Nigel Bunnett and Dr Elva Zhao (Monash Institute of Pharmaceutical Sciences) for assistance with calcium mobilisation assays. No author has a conflict of interest.

TABLE 1: Oligonucleotide primers

Name	***Forward (5'-3')***	***Reverse (5'-3')***
CD11b	CATCAAGGGCAGCCAGATTG	GAGGCAAGGGACACACTGAC
Cre	ATCTGGCATTTCTGGGGATTG	GGCAACACCATTTTTTCTGACC
Ifng	CAGCAACAGCAAGGCGAAA	CTGGACCTGTGGGTTGTTGAC
Il1b	GAAAGACGGCACACCCACC	AGACAAACCGTTTTTCCATCTTC
Il6	GAGCCCACCAAGAACGATAG	TCAGTCCCAAGAAGGCAACT
Mpo	CCGCCTGAACAATCAGTACC	ATTCTGGCGATTCAGTTTGG
Nos2	GAGGCCCAGGAGGAGAGAGATCCG	TCCATGCAGACAACCTTGGTGTTG
P. gingivalis-specific 16S rDNA	TGCAACTTGCCTTACAGAGGG	TCAGTTCCCCTACCCATCGT
Universal 16S rDNA	TCCTACGGGAGGCAGCAGT	GGACTACCAGGGTATCTAATCCTGTT

FIGURE LEGENDS

Figure 1: Characterisation of keratinocyte-specific PAR_2-null mice

A. Quantitative PCR analysis of *F2rl1* exon 2 in genomic DNA and *F2rl1* transcript in RNA isolated from keratinocytes from the skin of newborn *K14-Cre:F2rl1*$^{wt/wt}$ and *K14-Cre:F2rl1*$^{fl/fl}$ mice; *** $P < 0.001$. MNE – mean normalised expression. B. Calcium mobilisation assays conducted on keratinocytes and fibroblasts isolated from the skin of *K14-Cre:F2rl1*$^{wt/wt}$ and *K14-Cre:F2rl1*$^{fl/fl}$ mice, treated with vehicle alone (negative control), ATP (positive control) and the PAR_2 agonists, 2-furoyl-LIGRLO-NH_2 (2f-LI) and SLIGRL-NH_2 (SLI).

Figure 2: The periodontal disease model in global PAR_2-null and control strains of mice: confirmation of *P. gingivalis* infection and morphological changes

Samples were obtained from wildtype (*F2rl1*$^{wt/wt}$), non-Cre PAR_2 'floxed' (*F2rl1*$^{fl/fl}$) and global PAR_2-null (*F2rl1*$^{-/-}$) mice subjected to sham and Lig+Inf treatments. A. Quantification of *P. gingivalis* cells in gingiva and *P. gingivalis*-specific IgG in serum; Mann-Whitney test. B. Upper panel - three-dimensional reconstructions of microCT images of half maxillae. Lower panel - BV/TV values; Student's t-test. C. Quantification of osteoclasts in cryosections of maxillae stained for the presence of TRAP. Upper panel – micrographs of sections from *F2rl1*$^{wt/wt}$ mice, showing osteoclasts (multinucleate TRAP-positive cells; arrows); AB – alveolar bone, T – tooth, PL – periodontal ligament; bar = 100 μm. Lower panel – osteoclast counts (TRAP-positive cells/mm^2 of alveolar bone) in the three genotypes; Student's t-test. D. Quantification of mast cells in cryosections of maxillae; Student's t-test.

For comparisons between sham and Lig+Inf within genotypes: * P < 0.05, ** P < 0.01, *** P < 0.001, ns – no significant difference. For comparisons between *F2rl1*$^{wt/wt}$ and *F2rl1*$^{-/-}$ within treatments: # P < 0.05. For comparisons between *F2rl1*$^{fl/fl}$ and *F2rl1*$^{-/-}$ within treatments: ^ P < 0.05. Where there is no indication of a difference between genotypes, the difference was not significant.

Figure 3: The periodontal disease model in global PAR_2-null and control strains of mice: gene expression in gingival tissue

Quantitative PCR analysis of expression of *Il1b, Il6, Ifng, Mpo, Nos2* and *Cd11b* in gingival tissue from wildtype (*F2rl1*$^{wt/wt}$), non-Cre PAR_2 'floxed' (*F2rl1*$^{fl/fl}$) and global PAR_2-null (*F2rl1*$^{-/-}$) mice subjected to sham and Lig+Inf treatments. For comparisons between sham and Lig+Inf within genotypes: ** P < 0.01, *** P < 0.001, ns – no significant difference. For comparisons between *F2rl1*$^{wt/wt}$ and *F2rl1*$^{-/-}$ within treatments: ## P < 0.01, ### P < 0.001. For comparisons between *F2rl1*$^{fl/fl}$ and *F2rl1*$^{-/-}$ within treatments: ^^ P < 0.01, ^^^ P < 0.001. Where there is no indication of a difference between genotypes, the difference was not significant. MNE – mean normalised expression.

Figure 4: The periodontal disease model in keratinocyte-specific PAR_2-null mice: confirmation of *P. gingivalis* infection and morphological changes

Samples were obtained from *K14-Cre:F2rl1*$^{wt/wt}$ and *K14-Cre:F2rl1*$^{fl/fl}$ mice subjected to sham and Lig+Inf treatments. A. Quantification of *P. gingivalis* cells in gingiva and *P. gingivalis*-specific IgG in serum; Kruskal-Wallis test with Dunn's multiple comparison test.

B. Upper panel - three-dimensional reconstructions of microCT images of half maxillae. Lower panel - BV/TV values; two-way ANOVA with Sidak's multiple comparison test. C. Quantification of osteoclasts in cryosections of maxillae from *F2rl1*$^{wt/wt}$ mice, stained for the presence of TRAP; two-way ANOVA with Sidak's multiple comparison test. D. Quantification of mast cells in cryosections of maxillae; two-way ANOVA with Sidak's multiple comparison test. E. Determination of IL-6 concentration in serum; two-way ANOVA with Sidak's multiple comparison test. For comparisons between sham and Lig+Inf within genotypes: * $P < 0.05$, ** $P < 0.01$, ns – no significant difference. For comparisons between *K14-Cre:F2rl1*$^{wt/wt}$ and *K14-Cre:F2rl1*$^{fl/fl}$ within treatments: # $P < 0.05$. Where there is no indication of a difference between genotypes, the difference was not significant.

Figure 5: The periodontal disease model in keratinocyte-specific PAR_2-null mice: gene expression in gingival tissue

Quantitative PCR analysis of expression of *Il1b, Il6, Ifng, Mpo, Nos2* and *Cd11b* in gingival tissue from *K14-Cre:F2rl1*$^{wt/wt}$ and *K14-Cre:F2rl1*$^{fl/fl}$ mice subjected to sham and Lig+Inf treatments. For comparisons between sham and Lig+Inf within genotypes: * $P < 0.05$, ** $P < 0.01$, *** $P < 0.001$, ns – no significant difference. For comparisons between *K14-Cre:F2rl1*$^{wt/wt}$ and *K14-Cre:F2rl1*$^{fl/fl}$ within treatments: ## $P < 0.01$, ### $P < 0.001$. Where there is no indication of a difference between genotypes, the difference was not significant. MNE – mean normalised expression.

Figure 6: Schematic diagram illustrating our current understanding of the role of PAR_2 in the pathophysiology of periodontal disease

When gingival epithelial cells are exposed to *P. gingivalis*-derived proteases, PAR_2 on their surface is activated, leading to release of IL-6 and possibly other mediators, which in turn leads to infiltration of inflammatory cells, most likely macrophages and lymphocytes (shown here), as well as neutrophils. These cells in turn produce factors capable of stimulating osteoclast differentiation and activity and thus bone resorption. A second PAR_2-mediated pro-inflammatory pathway appears to exist, which leads to mast cell infiltration; this may involve secretion of HGF by gingival fibroblasts in response to activation of PAR_2 by *P. gingivalis* proteases. This pathway does not lead to bone resorption in the absence of PAR_2 on gingival epithelium, but may contribute to IL-1β-induced bone resorption through mast cell-derived nitric oxide (NO), when epithelial PAR_2 is present.

Supplementary Figure 1: The region of interest for determination of BV/TV in microCT images

A microCT slice of a half maxilla oriented in the dorsal plane, with the region of interest for determination of BV/TV outlined in yellow. The mesial (left side of image) and distal (right side of image) limits of the region of interest are indicated with white lines. M1, M2, M3 – the roots of molars 1-3.

REFERENCES

Abe, T., and Hajishengallis, G. (2013) Optimization of the ligature-induced periodontitis model in mice. *J Immunol Methods* **394**: 49-54.

Abraham, L.A., Chinni, C., Jenkins, A.L., Lourbakos, A., Ally, N., Pike, R.N., and Mackie, E.J. (2000) Expression of protease-activated receptor-2 by osteoblasts. *Bone* **26**: 7-14.

Adams, M.N., Ramachandran, R., Yau, M.K., Suen, J.Y., Fairlie, D.P., Hollenberg, M.D., and Hooper, J.D. (2011) Structure, function and pathophysiology of protease activated receptors. *Pharmacol Ther* **130**: 248-282.

Alshurafa, H.N., Stenton, G.R., Wallace, J.L., Hollenberg, M.D., Befus, A.D., and Vliagoftis, H. (2004) A protease activated receptor-2 (PAR-2) activating peptide, tc-LIGRLO-NH2, induces protease release from mast cells: role in TNF degradation. *BMC Pharmacol* **4**: 12.

Baker, P.J., Dixon, M., and Roopenian, D.C. (2000) Genetic control of susceptibility to Porphyromonas gingivalis-induced alveolar bone loss in mice. *Infect Immun* **68**: 5864-5868.

Bar-Shavit, R., Maoz, M., Yongjun, Y., Groysman, M., Dekel, I., and Katzav, S. (2002) Signalling pathways induced by protease-activated receptors and integrins in T cells. *Immunology* **105**: 35-46.

Belibasakis, G.N., Bostanci, N., and Reddi, D. (2010) Regulation of protease-activated receptor-2 expression in gingival fibroblasts and Jurkat T cells by Porphyromonas gingivalis. *Cell Biol Int* **34**: 287-292.

Bostanci, N., and Belibasakis, G.N. (2012) Porphyromonas gingivalis: an invasive and evasive opportunistic oral pathogen. *FEMS Microbiol Lett* **333**: 1-9.

Campbell, T.M., Wong, W.T., and Mackie, E.J. (2003) Establishment of a model of cortical bone repair in mice. *Calcif Tissue Int* **73**: 49-55.

Carvalho, R.F., Nilsson, G., and Harvima, I.T. (2010) Increased mast cell expression of PAR-2 in skin inflammatory diseases and release of IL-8 upon PAR-2 activation. *Exp Dermatol* **19**: 117-122.

D'Aiuto, F., Parkar, M., Andreou, G., Suvan, J., Brett, P.M., Ready, D., and Tonetti, M.S. (2004) Periodontitis and systemic inflammation: control of the local infection is associated with a reduction in serum inflammatory markers. *J Dent Res* **83**: 156-160.

D'Andrea, M.R., Rogahn, C.J., and Andrade-Gordon, P. (2000) Localization of protease-activated receptors-1 and -2 in human mast cells: indications for an amplified mast cell degranulation cascade. *Biotech Histochem* **75**: 85-90.

Fehlner-Gardiner, C.C., Cao, H., Jackson-Boeters, L., Nakamura, T., Elliott, B.E., Uniyal, S., and Chan, B.M. (1999) Characterization of a functional relationship between hepatocyte growth factor and mouse bone marrow-derived mast cells. *Differentiation* **65**: 27-42.

Francis, N., Every, A.L., Ayodele, B.A., Pike, R.N., Mackie, E.J., and Pagel, C.N. (2017) A T cell-specific knockout reveals an important role for protease-activated receptor 2 in lymphocyte development. *Int J Biochem Cell Biol* **92**: 95-103.

Georgy, S.R., Pagel, C.N., Wong, D.M., Sivagurunathan, S., Loh, L.H., Myers, D.E., Hollenberg, M.D., Pike, R.N., and Mackie, E.J. (2010) Proteinase-activated receptor-

2 (PAR2) and mouse osteoblasts: regulation of cell function and lack of specificity of PAR2-activating peptides. *Clin Exp Pharmacol Physiol* **37**: 328-336.

Grenier, D., and Grignon, L. (2006) Response of human macrophage-like cells to stimulation by Fusobacterium nucleatum ssp. nucleatum lipopolysaccharide. *Oral Microbiol Immunol* **21**: 190-196.

Gully, N., Bright, R., Marino, V., Marchant, C., Cantley, M., Haynes, D., Butler, C., Dashper, S., Reynolds, E., and Bartold, M. (2014) Porphyromonas gingivalis peptidylarginine deiminase, a key contributor in the pathogenesis of experimental periodontal disease and experimental arthritis. *PLoS One* **9**: e100838.

Herrera, B.S., Martins-Porto, R., Maia-Dantas, A., Campi, P., Spolidorio, L.C., Costa, S.K., Van Dyke, T.E., Gyurko, R., and Muscara, M.N. (2011) iNOS-derived nitric oxide stimulates osteoclast activity and alveolar bone loss in ligature-induced periodontitis in rats. *J Periodontol* **82**: 1608-1615.

Holzhausen, M., Spolidorio, L.C., Ellen, R.P., Jobin, M.C., Steinhoff, M., Andrade-Gordon, P., and Vergnolle, N. (2006) Protease-activated receptor-2 activation: a major role in the pathogenesis of Porphyromonas gingivalis infection. *Am J Pathol* **168**: 1189-1199.

Holzhausen, M., Spolidorio, L.C., and Vergnolle, N. (2005) Proteinase-activated receptor-2 (PAR2) agonist causes periodontitis in rats. *J Dent Res* **84**: 154-159.

Huelsken, J., Vogel, R., Erdmann, B., Cotsarelis, G., and Birchmeier, W. (2001) beta-Catenin controls hair follicle morphogenesis and stem cell differentiation in the skin. *Cell* **105**: 533-545.

Kayal, R.A. (2013) The role of osteoimmunology in periodontal disease. *Biomed Res Int* **2013**: 639368.

Lappin, D.F., Kjeldsen, M., Sander, L., and Kinane, D.F. (2000) Inducible nitric oxide synthase expression in periodontitis. *J Periodontal Res* **35**: 369-373.

Lichti, U., Anders, J., and Yuspa, S.H. (2008) Isolation and short-term culture of primary keratinocytes, hair follicle populations and dermal cells from newborn mice and keratinocytes from adult mice for in vitro analysis and for grafting to immunodeficient mice. *Nat Protoc* **3**: 799-810.

Lin, J., Bi, L., Yu, X., Kawai, T., Taubman, M.A., Shen, B., and Han, X. (2014) Porphyromonas gingivalis exacerbates ligature-induced, RANKL-dependent alveolar bone resorption via differential regulation of Toll-like receptor 2 (TLR2) and TLR4. *Infect Immun* **82**: 4127-4134.

Lindner, J.R., Kahn, M.L., Coughlin, S.R., Sambrano, G.R., Schauble, E., Bernstein, D., Foy, D., Hafezi-Moghadam, A., and Ley, K. (2000) Delayed onset of inflammation in protease-activated receptor-2-deficient mice. *J Immunol* **165**: 6504-6510.

Liu, Y., Wu, Z., Nakanishi, Y., Ni, J., Hayashi, Y., Takayama, F., Zhou, Y., Kadawaki, T., and Nakanishi, H. (2017) Infection of microglia with Porphyromonas gingivalis promotes cell migration and an inflammatory response through the gingipain-mediated activation of protease-activated receptor-2 in mice. *Sci Rep* **7**: 11759.

Lohinai, Z., Benedek, P., Feher, E., Gyorfi, A., Rosivall, L., Fazekas, A., Salzman, A.L., and Szabo, C. (1998) Protective effects of mercaptoethylguanidine, a selective inhibitor of

inducible nitric oxide synthase, in ligature-induced periodontitis in the rat. *Br J Pharmacol* **123**: 353-360.

Loos, B.G., Craandijk, J., Hoek, F.J., Wertheim-van Dillen, P.M., and van der Velden, U. (2000) Elevation of systemic markers related to cardiovascular diseases in the peripheral blood of periodontitis patients. *J Periodontol* **71**: 1528-1534.

Lourbakos, A., Chinni, C., Thompson, P., Potempa, J., Travis, J., Mackie, E.J., and Pike, R.N. (1998) Cleavage and activation of proteinase-activated receptor-2 on human neutrophils by gingipain-R from Porphyromonas gingivalis. *FEBS Lett* **435**: 45-48.

Lourbakos, A., Potempa, J., Travis, J., D'Andrea, M.R., Andrade-Gordon, P., Santulli, R., Mackie, E.J., and Pike, R.N. (2001) Arginine-specific protease from Porphyromonas gingivalis activates protease-activated receptors on human oral epithelial cells and induces interleukin-6 secretion. *Infect Immun* **69**: 5121-5130.

Lundqvist, C., Baranov, V., Teglund, S., Hammarstrom, S., and Hammarstrom, M.L. (1994) Cytokine profile and ultrastructure of intraepithelial gamma delta T cells in chronically inflamed human gingiva suggest a cytotoxic effector function. *J Immunol* **153**: 2302-2312.

Malcolm, J., Millington, O., Millhouse, E., Campbell, L., Adrados Planell, A., Butcher, J.P., Lawrence, C., Ross, K., Ramage, G., McInnes, I.B., and Culshaw, S. (2016) Mast Cells Contribute to Porphyromonas gingivalis-induced Bone Loss. *J Dent Res* **95**: 704-710.

Moormann, C., Artuc, M., Pohl, E., Varga, G., Buddenkotte, J., Vergnolle, N., Brehler, R., Henz, B.M., Schneider, S.W., Luger, T.A., and Steinhoff, M. (2006) Functional characterization and expression analysis of the proteinase-activated receptor-2 in human cutaneous mast cells. *J Invest Dermatol* **126**: 746-755.

O'Brien-Simpson, N.M., Black, C.L., Bhogal, P.S., Cleal, S.M., Slakeski, N., Higgins, T.J., and Reynolds, E.C. (2000a) Serum immunoglobulin G (IgG) and IgG subclass responses to the RgpA-Kgp proteinase-adhesin complex of Porphyromonas gingivalis in adult periodontitis. *Infect Immun* **68**: 2704-2712.

O'Brien-Simpson, N.M., Paolini, R.A., Hoffmann, B., Slakeski, N., Dashper, S.G., and Reynolds, E.C. (2001) Role of RgpA, RgpB, and Kgp proteinases in virulence of Porphyromonas gingivalis W50 in a murine lesion model. *Infect Immun* **69**: 7527-7534.

O'Brien-Simpson, N.M., Paolini, R.A., and Reynolds, E.C. (2000b) RgpA-Kgp peptide-based immunogens provide protection against Porphyromonas gingivalis challenge in a murine lesion model. *Infect Immun* **68**: 4055-4063.

Pagel, C.N., de Niese, M.R., Abraham, L.A., Chinni, C., Song, S.J., Pike, R.N., and Mackie, E.J. (2003) Inhibition of osteoblast apoptosis by thrombin. *Bone* **33**: 733-743.

Palm, E., Khalaf, H., and Bengtsson, T. (2013) Porphyromonas gingivalis downregulates the immune response of fibroblasts. *BMC Microbiol* **13**: 155.

Pathirana, R.D., O'Brien-Simpson, N.M., Brammar, G.C., Slakeski, N., and Reynolds, E.C. (2007) Kgp and RgpB, but not RgpA, are important for Porphyromonas gingivalis virulence in the murine periodontitis model. *Infect Immun* **75**: 1436-1442.

Pfaffl, M.W., Horgan, G.W., and Dempfle, L. (2002) Relative expression software tool (REST) for group-wise comparison and statistical analysis of relative expression results in real-time PCR. *Nucleic Acids Res* **30**: e36.

Ramachandran, R., Mihara, K., Chung, H., Renaux, B., Lau, C.S., Muruve, D.A., DeFea, K.A., Bouvier, M., and Hollenberg, M.D. (2011) Neutrophil elastase acts as a biased agonist for proteinase-activated receptor-2 (PAR2). *J Biol Chem* **286**: 24638-24648.

Shpacovitch, V.M., Varga, G., Strey, A., Gunzer, M., Mooren, F., Buddenkotte, J., Vergnolle, N., Sommerhoff, C.P., Grabbe, S., Gerke, V., Homey, B., Hollenberg, M., Luger, T.A., and Steinhoff, M. (2004) Agonists of proteinase-activated receptor-2 modulate human neutrophil cytokine secretion, expression of cell adhesion molecules, and migration within 3-D collagen lattices. *J Leukoc Biol* **76**: 388-398.

Simon, P. (2003) Q-Gene: processing quantitative real-time RT-PCR data. *Bioinformatics* **19**: 1439-1440.

Smith, R., Ransjo, M., Tatarczuch, L., Song, S.J., Pagel, C., Morrison, J.R., Pike, R.N., and Mackie, E.J. (2004) Activation of protease-activated receptor-2 leads to inhibition of osteoclast differentiation. *J Bone Miner Res* **19**: 507-516.

Truett, G.E., Heeger, P., Mynatt, R.L., Truett, A.A., Walker, J.A., and Warman, M.L. (2000) Preparation of PCR-quality mouse genomic DNA with hot sodium hydroxide and tris (HotSHOT). *Biotechniques* **29**: 52, 54.

Uehara, A., Muramoto, K., Imamura, T., Nakayama, K., Potempa, J., Travis, J., Sugawara, S., and Takada, H. (2005) Arginine-specific gingipains from Porphyromonas gingivalis stimulate production of hepatocyte growth factor (scatter factor) through protease-activated receptors in human gingival fibroblasts in culture. *J Immunol* **175**: 6076-6084.

van't Hof, R.J., Armour, K.J., Smith, L.M., Armour, K.E., Wei, X.Q., Liew, F.Y., and Ralston, S.H. (2000) Requirement of the inducible nitric oxide synthase pathway for IL-1-induced osteoclastic bone resorption. *Proc Natl Acad Sci U S A* **97**: 7993-7998.

Wong, D.M., Tam, V., Lam, R., Walsh, K.A., Tatarczuch, L., Pagel, C.N., Reynolds, E.C., O'Brien-Simpson, N.M., Mackie, E.J., and Pike, R.N. (2010) Protease-activated receptor 2 has pivotal roles in cellular mechanisms involved in experimental periodontitis. *Infect Immun* **78**: 629-638.

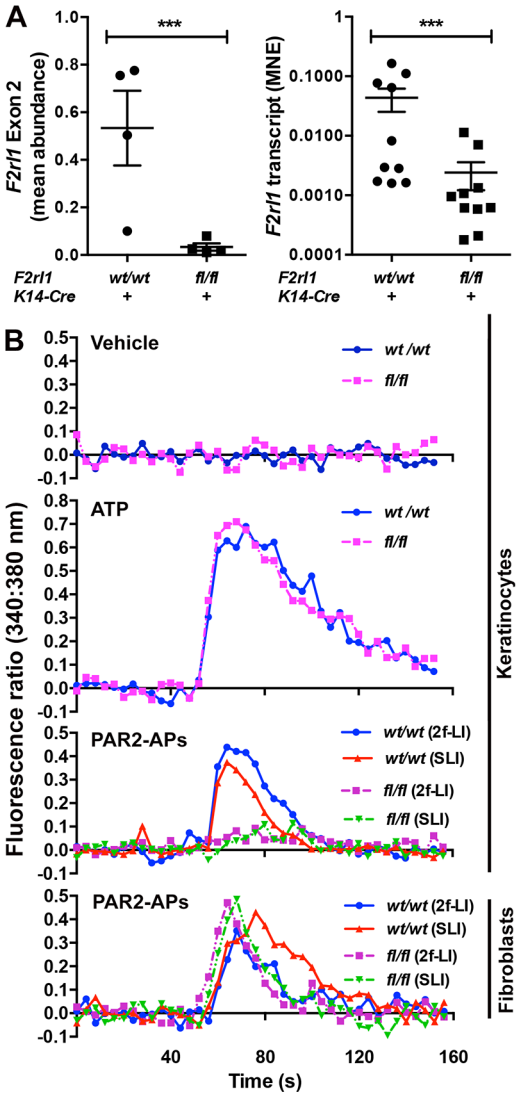

CMI_12891_F1.tif

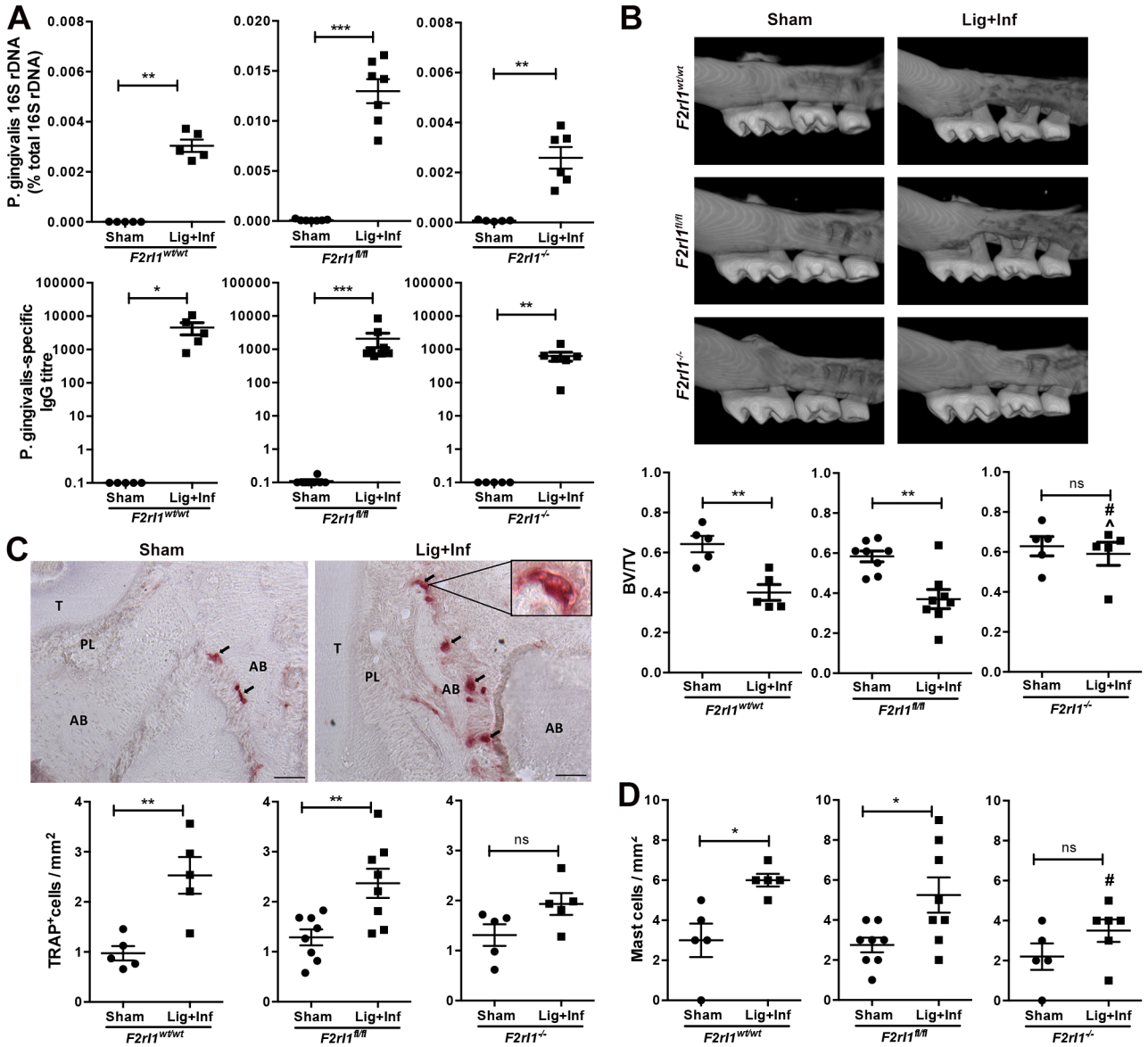

CMI_12891_F2.tif

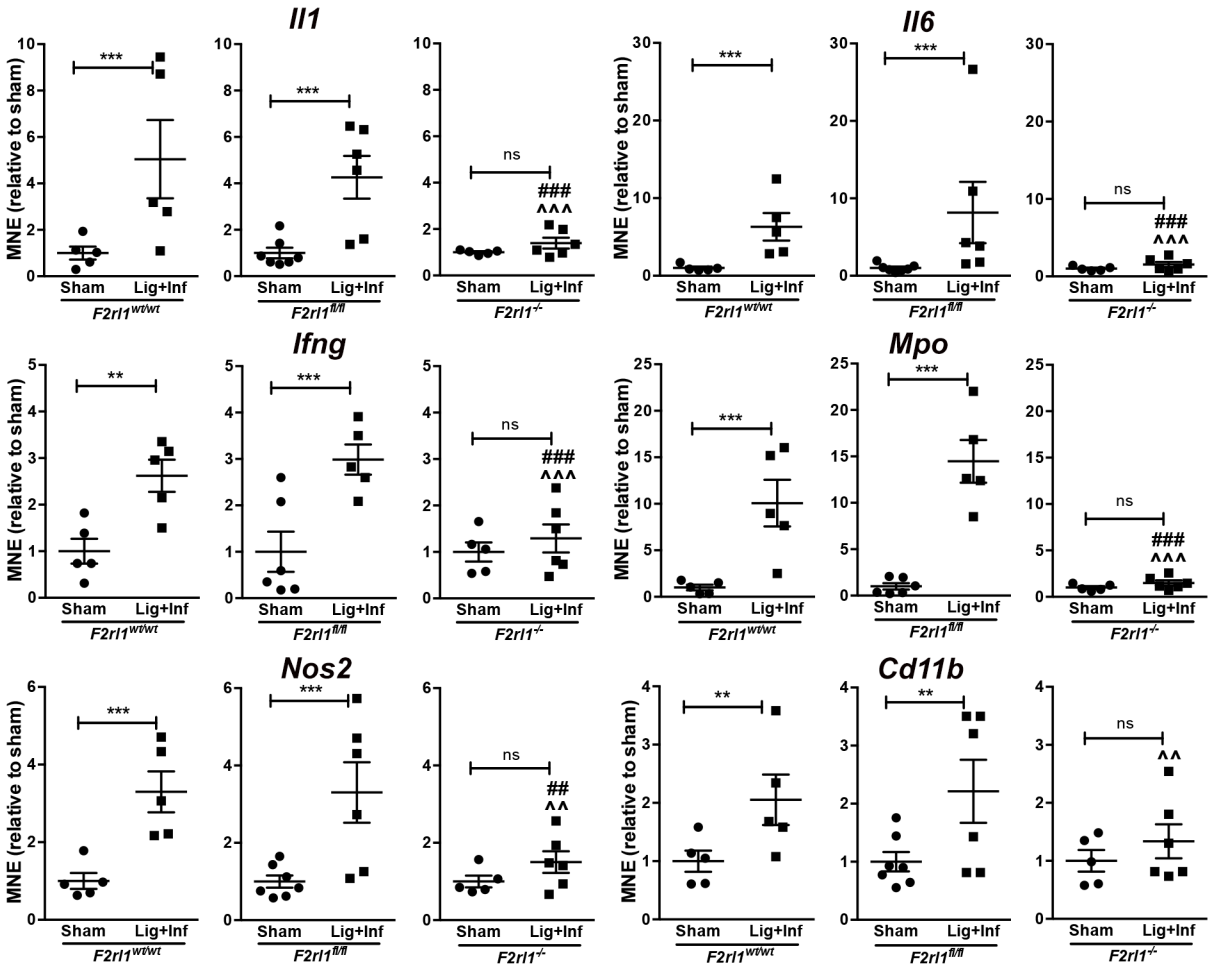

CMI_12891_F3.tif

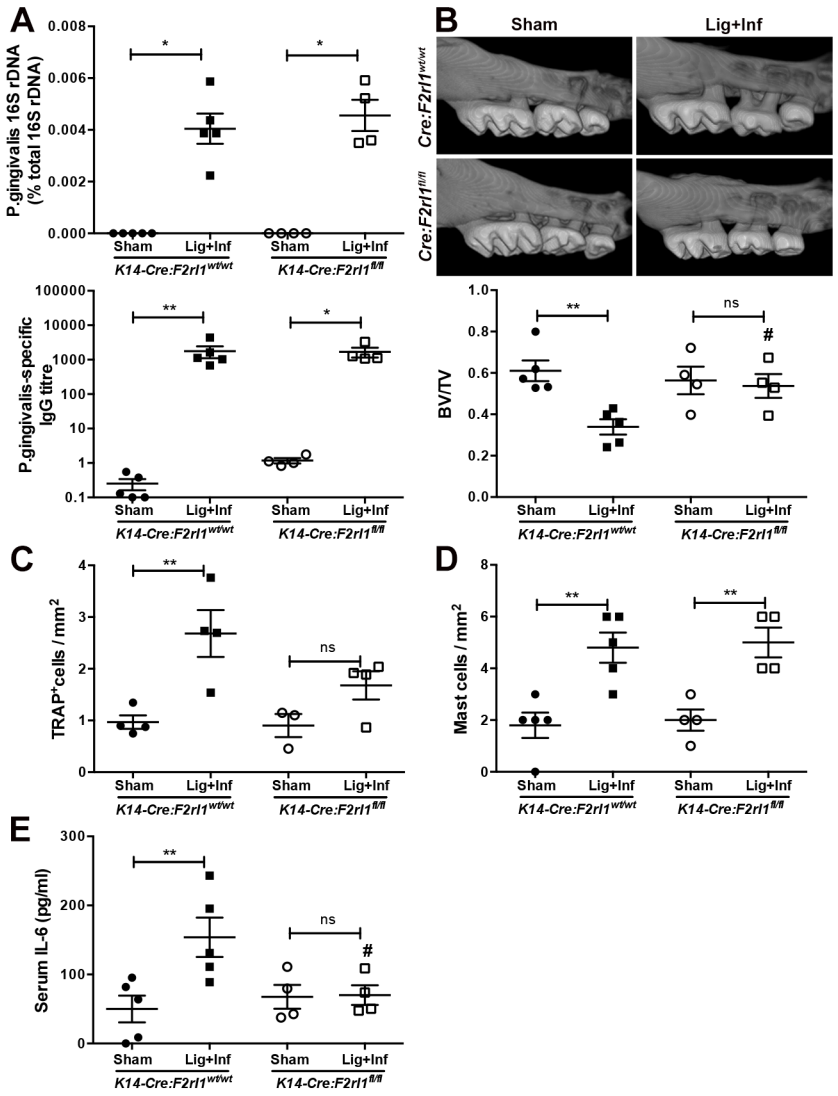

CMI_12891_F4.tif

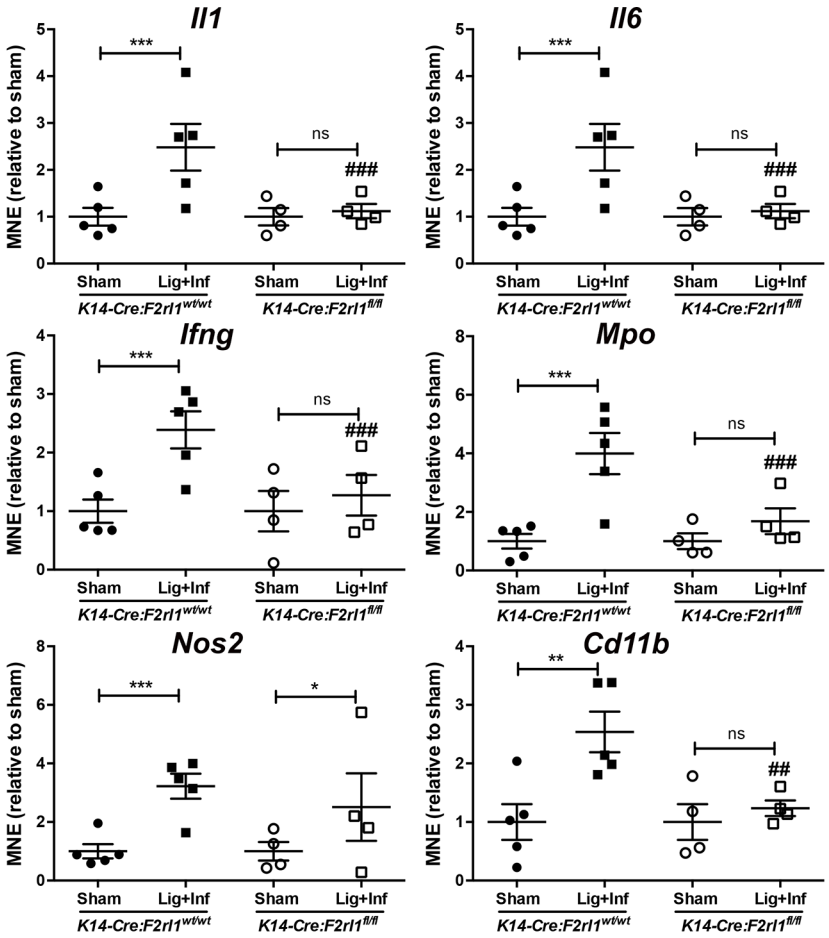

CMI_12891_F5.tif

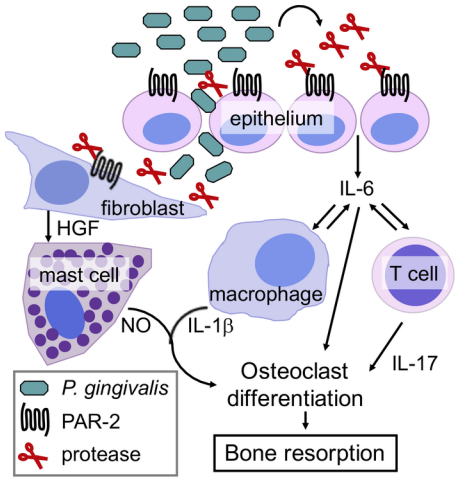

CMI_12891_F6.tif